https://rbgeomorfologia.org.br/
ISSN 2236-5664

Revista Brasileira de Geomorfologia

v. 26, nº 4 (2025)

http://dx.doi.org/10.20502/rbg.v26i4.2677

Research Article

Determination of Coastal Erosion Rate from Multitemporal Landsat Data at Barra Beach, Southern Mozambique

Determinação da taxa de erosão costeira a partir de dados multitemporais da série Landsat na Praia da Barra, Sul de Moçambique

Oldim Lodes Agostinho C. Vilanculo [1], Hélder Arlindo Machaieie [2]

[1] Eduardo Mondlane University (UEM), Escola Superior de Ciências Marinhas e Costeiras, Quelimane, Mozambique. ochuquelane@gmail.com.
ORCID: https://orcid.org/0000-0001-5991-1085

[2] Eduardo Mondlane University (UEM), Escola Superior de Ciências Marinhas e Costeiras, Quelimane, Mozambique. machaielder@gmail.com.
ORCID: https://orcid.org/0000-0002-9461-4905

Received: 19/02/2025; Accepted: 01/10/2025; Published: 12/11/2025

Abstract: This study analyzes the shoreline dynamics at Barra Beach, located in southern Mozambique, over a 24-year period. The main objectives were to quantify rates of coastal accretion and erosion and to identify key drivers of shoreline retreat. We utilized Landsat imagery, processed with the Google Earth Engine (GEE), to generate annual median composites, from which shoreline positions were extracted. These were then analyzed using the Digital Shoreline Analysis System (DSAS), applying the Weighted Linear Regression (WLR) method to compute rates of change. Our results indicate that 65.4% of transects exhibit erosion, with an average shoreline retreat rate of –2.72 m/yr (standard deviation of 3.18 m/yr). In contrast, 34.6% exhibit accretion, with an average progradation of 1.48 m/yr (standard deviation of 2.57 m/yr). The most extreme erosion rates (WLR = –11.02 m/yr) occurred in zones of intense tourism, where dune vegetation removal has compromised the natural buffer against marine intrusion. In conclusion, Barra Beach is undergoing predominantly erosional processes, albeit with considerable spatial variability. These findings underscore the urgent need for targeted mitigation strategies to enhance the region's coastal resilience and to preserve its environmental integrity.

Keywords: Coastal geomorphology, Shoreline, Google Earth Engine, Digital Shoreline Analysis System (DSAS).

Resumo: A presente pesquisa analisou a dinâmica da linha de costa (LC) na Praia da Barra, sul de Moçambique, ao longo de 24 anos, com o objetivo de avaliar as taxas de avanço e recuo da linha costeira e identificar os fatores associados à erosão. Foram utilizadas imagens Landsat processadas no *Google Earth Engine* (GEE) para a criação de composições medianas anuais, seguidas da extração das linhas de costa e análise no *Digital Shoreline Analysis System* (DSAS), aplicando o método *Weighted Linear Regression Rate* (WLR). Os resultados indicaram que 65,4% dos transectos apresentaram erosão, com taxa média de recuo de -2,72 m/ano (desvio padrão de 3,18 m/ano), enquanto 34,6% evidenciaram deposição, com taxa média de avanço de 1,48 m/ano (desvio padrão de 2,57 m/ano). As maiores taxas negativas de WLR (-11,02 m/ano) ocorreram em áreas de intensa atividade turística, onde a remoção da vegetação das dunas reduziu a proteção natural contra o avanço do mar. Conclui-se que a Praia da Barra apresenta predominância de processos erosivos, com elevada variabilidade espacial, o que reforça a necessidade urgente de implementação de estratégias de mitigação que aumentem a resiliência ambiental da região.

Palavras-chave: Geomorfologia costeira, Linha de costa, Google Earth Engine, Digital Shoreline Analysis System (DSAS).

1. Introduction

The shoreline, that is, the boundary between land and sea, is in a constant state of change in both form and location due to dynamic environmental conditions (Prasad; Kumar, 2014). In its classical definition, the shoreline is understood as the approximate position of the mean high-water line, identified by the High Water Line (HWL), which is considered the most consistent and widely applicable indicator in studies of historical coastal change (Crowell; Leatherman; Buckley, 1991). Therefore, shoreline movement reflects the interaction between marine and terrestrial processes that shape and reshape the coastal margin. Although fundamentally a natural phenomenon, this movement can become problematic when coastal erosion threatens the safety of populations, ecosystems, and infrastructure located in coastal zones—thus constituting a global challenge that affects practically every country with a coastline (Pajak; Idzikowska; Kowalczyk, 2024).

A global study published by the European Commission revealed that nearly half of the world's sandy beaches could disappear by the end of the century due primarily to sea-level rise, while also highlighting regions—such as the Amazon and parts of East and Southeast Asia—where erosion is offset by natural sediment accumulation (Vousdoukas et al., 2020). Along the eastern African coast—including countries bordering the Indian Ocean—sea-level rise has profound and real consequences. It is expected to induce tidal flooding, initiate or exacerbate coastal erosion, inhibit natural coastal drainage, and increase saline intrusion into important freshwater aquifers and agricultural lands (Okemwa, 1992).

Global mean sea level has risen by 20 to 25 cm since 1900, with an impressive half of that increase occurring since 1980. The rate of this rise has also accelerated significantly—from 1.5 mm per year (1901–1990) to 3.6 mm per year (2005–2015) (Oppenheimer et al., 2019; IPCC, 2021). Along the African coast, regional sea-level rise rates have deviated markedly from the global average, ranging from 2.48 to 5.44 mm per year between 1993 and 2022 (Pajak; Idzikowska; Kowalczyk, 2024). Beyond the combined effects of sea-level rise and storms, anthropogenic activity has made the continuous change in shoreline form and position a subject of numerous studies (Fan; Xu; Wu; Lee, 2019). The removal of natural barriers such as mangroves significantly increases coastal vulnerability to erosion and storm impact (Nguyen et al., 2015).

Mozambique's extensive coastline—of great socio-cultural and economic importance—is among the most vulnerable to coastal erosion due to extreme metoceanographic events, particularly storms and tropical cyclones, as well as human activity (Massuanganhe; Arnberg, 2008; Cabral et al., 2017). This human activity, characterized by the destruction of native coastal vegetation and poor infrastructure construction, has accelerated erosion in some regions of the country (Hoguane, 2007).

At Barra Beach, in southern Mozambique, studies indicate that coastal erosion has impacted both the natural environment and local infrastructure (Azevedo; Frei; Marques, 2013). In this region, erosion has been aggravated by the clearing of native dune vegetation—mainly due to the expansion of tourism developments and coastal infrastructure—which has intensified shoreline instability (Palalane; Larson; Hanson; Juízo, 2016). As a consequence, buildings close to the beach face escalating risk as shoreline retreat subjects previously safe areas to flooding. However, despite its relevance for land-use planning and coastal hazard prevention, shoreline erosion and accretion rates have not been examined in detail.

Previous studies highlighted vegetation loss—due to tourism and coastal development—as a major factor exacerbating shoreline change at Barra Beach (Azevedo, 2009; Azevedo; Frei; Marques, 2013; Palalane; Larson; Hanson; Juízo, 2016). Nonetheless, quantitative, long-term data on shoreline advance and retreat rates across various sectors of the beach remain unknown.

Recent research has emphasized the use of GIS tools and remote sensing data for shoreline mapping (Pardo-Pascual et al., 2018; Bishop-Taylor; Nanson; Sagar; Lymburner, 2021; Spinosa et al., 2021). The integration of cloud-based platforms like Google Earth Engine (GEE) with long time-series of high- and medium-resolution imagery (such as Landsat), along with shoreline-dynamics tools like the Digital Shoreline Analysis System (DSAS), presents an effective alternative for shoreline monitoring (Christofi et al., 2025). However, this approach remains underutilized on Mozambique's beaches.

This research aims to analyze shoreline dynamics—advance or retreat, erosion and accretion—at Barra Beach over a 24-year period. The methodology is based on constructing annual temporal median composites in GEE, aiming to reduce error related to tidal data absence during shoreline extraction. This methodology enables derivation of a mean shoreline, which several authors (Almonacid-Caballer et al., 2016; Sayre et al., 2019; Vos et

al., 2019; Hu; Fan; Zhang, 2024) have indicated to be less sensitive to transient tidal, wind, or extreme weather variations. The outcomes can inform coastal policy and management strategies in Mozambique. Furthermore, the methodology applied in this study can be replicated for monitoring other beaches in the country, providing a solid foundation for future coastal management research and action.

2. Study Area

Barra Beach is situated in Inhambane Province, in southern Mozambique, approximately 20 km northeast of the city of Inhambane, on a peninsula that separates Inhambane Bay from the Indian Ocean (Figure 1). This beach is one of the principal tourist and recreational destinations in Inhambane Province, renowned for its crystal-clear waters, extensive coastal dune systems, and abundant marine life, including dolphins, rays, and whale sharks (Fernando, 2013; Fordyce, 2018). Notably, the Barra and Tofo area is recognized globally for opportunities to see whale sharks and manta rays.

The region experiences a tropical humid climate modified by elevation, characterized by cool, very rainy periods. Monthly mean maximum temperatures average around 26.97 °C, with minimums near 20.3 °C, and an annual average precipitation of approximately 926.8 mm (Zacarias, 2013). The locale is further influenced by coastal currents, swell, and occasionally tropical cyclones, which intensify coastal erosion and sediment dynamics, placing the area at increasing risk due to climate change and urban expansion (Palalane; Larson; Hanson; Juízo, 2016).

Barra Beach is characterized as a relatively exposed beach break (sandy bottom), meaning that wave formation is controlled by the shallow sandy seabed, resulting in inconsistent surf conditions. The region receives both groundswells (long-period waves generated by distant storms) and windswells (short-period waves produced by local winds near the coast), with the most favorable swell direction coming from the southeast (Surf-Forecast, 2025). The coastline is marked by strong currents typically flowing from northwest to southeast and is also the closest point to Inhambane Bay and the associated estuarine system (Kelchner et al., 2021). The astronomical tide is semidiurnal, with two high tides and two low tides each day, with amplitude reaching approximately 3 m (Hoguane, 2007). Surface currents (drifters) average between 0.3 and 0.5 m/s, and can intensify when influenced by external forcings such as tides, wind, waves, and eddies from the Mozambique Channel (Christensen et al., 2014).

The geology and geomorphology of Inhambane Province reflect the evolution of the Mozambique Basin since the Cretaceous, characterized by continental, marine, and transitional deposits overlain by thick Quaternary sequences of fluvial and aeolian origin (Dumouchel, Hees & Alvin, 2016). The beach geology is dominated by Quaternary sedimentary deposits, a common feature in southern Mozambique and along much of the coastline (Muchangos, 1999). The present geomorphology is dominated by a multigenerational field of paleodunes and active dunes, alluvial plains, and lagoonal zones, resulting from the interaction between sea-level fluctuations, fluvial processes, prevailing winds, and coastal currents (Dumouchel, Hees & Alvin, 2016). The region has a gently sloping profile, with the seabed descending to about 30 m at 3 km from the coast, followed by a steep drop to 60 m (Christensen et al., 2014). In addition, beachrock outcrops in the intertidal zone play a significant role in coastal dynamics by dissipating wave energy, retaining sediments transported predominantly northward by longshore currents, and exerting morphological control over the configuration of the shoreline (Matias, 2020).

3. Materials and Methods

In this research, we utilized surface reflectance images from Landsat 5, 7, and 8, all atmospherically corrected**.** From these Landsat images, we extracted shorelines over a period of 24 years, enabling the analysis of decadal-scale changes from 2000 to 2024. For each year in the analysis period, images were filtered by date (from January 1 to December 31) and cloud cover (less than 10%). Such selection criteria are particularly valuable for assessing trends in erosion, accretion**,** and alterations induced by human activity or climate change. The long-term shoreline history derived from these Landsat datasets allows for precise detection and continuous monitoring of coastal variations, as demonstrated in multiple studies (Almonacid-Caballer et al., 2016; Ferreira, 2019; Bishop-Taylor; Nanson; Sagar; Lymburner, 2021; Quang et al., 2021).

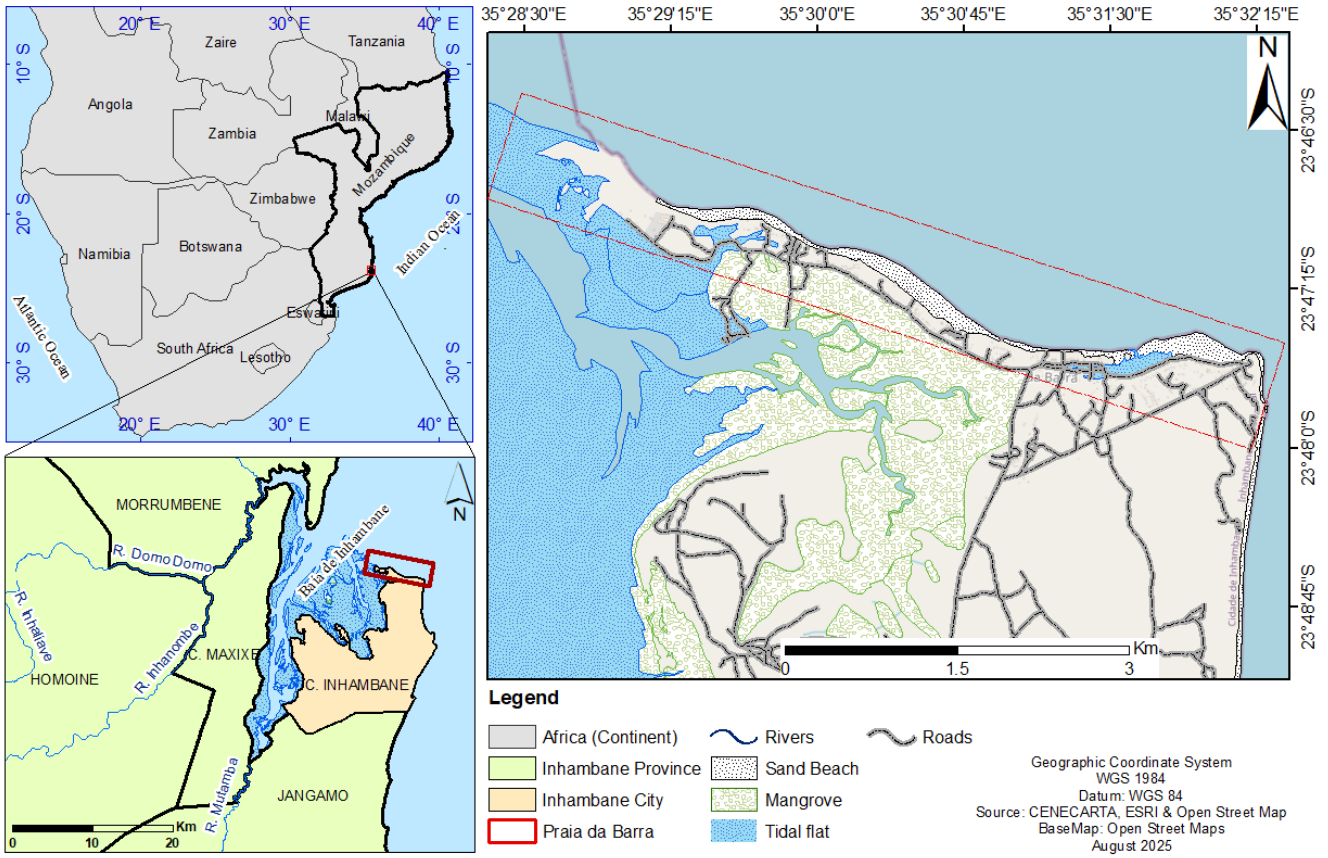

Figure 1. Geographic location of the study area.

3.1. Composites of satellite images

Accurate and continuous field survey data are essential for understanding shoreline evolution—but this requirement is often constrained by limited resources and manpower across many beaches (Hu; Fan; Zhang, 2024). To address the scarcity of field data, some studies have turned to long-term, continuous satellite imagery, such as Landsat and Sentinel series, to investigate decadal-scale shoreline change (Pardo-Pascual et al., 2018; Bishop-Taylor; Nanson; Sagar; Lymburner, 2021). The methodological workflow used in this study has been validated against field measurements as efficient (Vos et al., 2019).

The Google Earth Engine (GEE) platform provides a wide range of publicly accessible and continuously updated satellite datasets (Gorelick et al., 2017). All satellite images used in this research were seamlessly integrated within GEE. The use of this platform has gained prominence in shoreline monitoring by enabling image compositing to reduce errors induced by temporal variability—such as tidal fluctuations, cloud cover, and atmospheric distortions (Vos et al., 2019). In this study, we employed annual median image composites (Figure 2). The Global Shoreline Vector (GSV)—a global shoreline dataset derived from U.S. Geological Survey satellite imagery—uses annual median composites to generate coastal positions between the high and low tide lines (Sayre et al., 2019). The median filter is a statistical method that replaces each pixel's value with the median of its neighbourhood, allowing a representative annual image to be generated from a time series, thereby minimizing noise caused by temporal variabilities (Gorelick et al., 2017).

3.2. Shoreline Extraction

The Modified Normalized Difference Water Index (MNDWI) was employed to detect the wet/dry boundary at the ocean–land interface (Júnior; de Alencar Castro, 2024). This index performs well in delineating the land–water boundary, as evidenced by prior studies (Vos et al., 2019; Bishop-Taylor; Nanson; Sagar; Lymburner, 2021). The MNDWI is calculated using the following equation (Xu, 2006):

$$MNDWI = (Green - NIR)/(Green + NIR) \quad \text{(Eq. 1)}$$

Where *Green* represents the green spectral band and *NIR* is the near-infrared band.

Research by Günen and Atasever (2024), which evaluated the efficacy of various water indices (WRI, NWI, MNDWI, NDWI), found that the MNDWI consistently emerged as a robust tool for water extraction. In comparative studies, Hastuti; Ismail and Nagai (2024) further demonstrated that MNDWI is the most effective index for shoreline extraction.

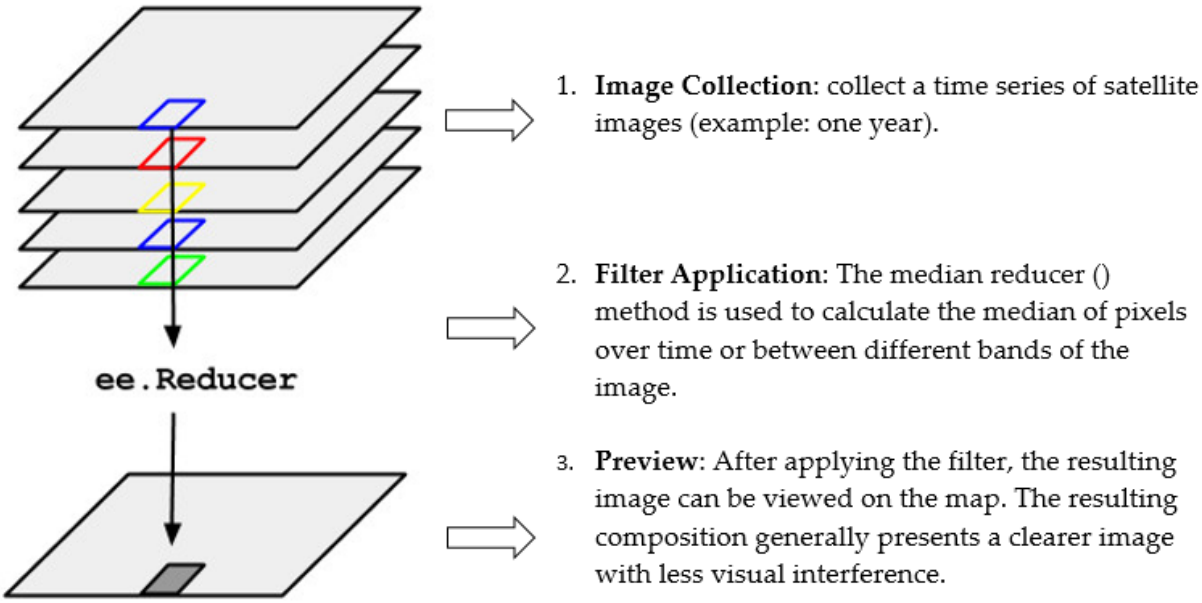

Figure 2. Principle of median filter in Google Earth Engine

The combination of MNDWI with Otsu's method offers an automatic approach for coastline extraction, wherein satellite images are processed to identify the interface between ocean and land (Donchyts et al., 2016). This approach yields a probability density function histogram of the resulting binary image (water vs. land) (Vos et al., 2019). We applied the Otsu Dynamic Thresholding method introduced by Donchyts et al. (2016), which develops an approach to derive a water mask from satellite imagery. The Otsu method enables fully.

3.3. Morphological Operation

Donchyts et al. (2016) applied the mathematical morphology method for hit-or-miss transformation to a binary water mask image. In this method, potential water and land pixels located near the water are then computed using dilation and morphological erosion applied to the detected edges. According to Spinosa et al. (2021), morphological operations are widely used in image processing because they clarify the image by eliminating irrelevancies and preserving the shape of objects. Extracted coastlines can be discontinuous, especially in tidal

areas or where image quality is poor. Dilation combines two vectors using addition, while erosion uses subtraction. In this study, we apply the morphological dilation operations.

3.4. Coastline Change Detection

The detection and analysis of shoreline changes over the 24-year study period was performed using the Digital Shoreline Analysis System (DSAS) tool. This is an extension of ArcGIS software, developed by the U.S. Geological Survey (USGS), which allows the calculation of rates of shoreline change based on time series of geospatial data (Himmelstoss et al., 2024). DSAS automatically generates lines perpendicular to the shoreline (transects) from a user-defined baseline. These lines are used to measure spatial changes in shoreline position. In DSAS, the End Point Rate (EPR) calculates shoreline change using only two dates, while the Linear Regression Rate (LRR) fits a linear regression considering multiple years, providing a more stable estimate.

Weighted Linear Regression (WLR) improves LRR by assigning weights to points based on their accuracy, making the analysis more reliable. These methods were applied in this research because they are efficient for studying coastal dynamics, as demonstrated in other studies (Ferreira, 2019; Estevam; Osako; Francisco, 2021; Quang et al., 2021). In this study, 81 transects were constructed perpendicular to the coast, with a 100-meter spacing between transects and a smoothing distance of 2,000 meters. The reliability of the simple linear regression (LRR) and weighted linear regression (WLR) models was assessed using the coefficient of determination (R^2), standard error, and 95% confidence interval.

4. Results

The temporal mean coastline represents the average position of the coastline over the course of a year (Figure 3). This average is derived from the analysis of multiple images acquired under different temporal conditions. In this research, we considered using the median, which is the central position of the data, divided into two equal parts. This function is useful in scenarios where there are extreme values or asymmetric distributions, such as coastline variations influenced by high tides, storms, or calm periods.

4.1. Uncertainties in the position of the coastline

Figure 3 shows the distribution of shoreline change rates for the methods: EPR (gray), LRR (dimgray), and WLR (white). The colors represent each method, and the black dashed line indicates the zero-change rate, which separates erosion areas (negative values) from accretion areas (positive values). Most values are concentrated on the negative side, indicating a predominance of erosion. In Figure 3, it can be observed that the results of the Weighted Linear Regression (WLR) method overlap with those of the Linear Regression Rate (LRR). For most transects, the coefficient of determination (R^2) yielded identical values for both models, meaning they explain the same proportion of data variability. Similarly, the 95% confidence interval (CI95) was also equivalent, indicating a 95% probability that the actual shoreline change rate lies within the estimated interval. The main difference between the models is associated with the standard error. In the case of WLR, the Weighted Standard Error (WSE) is used, which assigns greater weight to observations that are more representative of the temporal trend. Since the WSE was smaller for WLR than for LRR, the weighted model is considered to provide more reliable shoreline change rate estimates, reducing the effect of potential outliers.

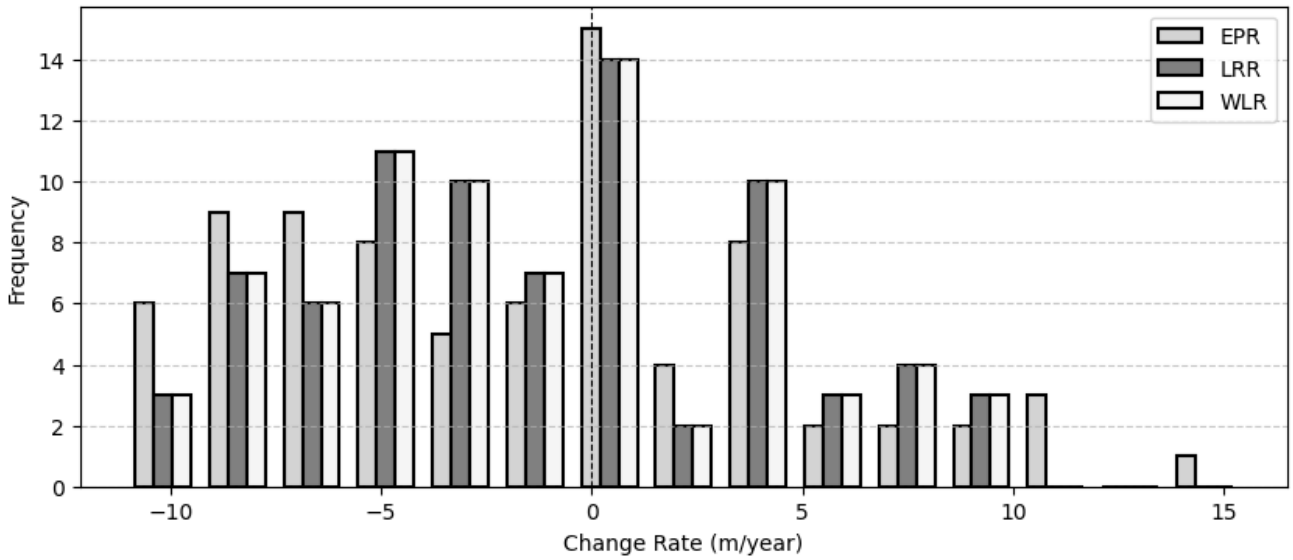

Figure 3. Distribution of Coastline Change Rates on Barra Beach.

From the WR2 data (R^2 of the weighted linear regression model) and WCI95 (95% confidence interval of the weighted model), the accuracy of each transect generated by the model was determined (Figure 4). Of the 82 transects analyzed, 20 presented high reliability (WR2 ≥ 0.7), 41 had medium reliability (0.3 ≤ WR2 < 0.7) and only 15 transects (3, 13, 14, 15, 16, 29, 30, 63, 64, 65, 66, 67, 69, 71, 72) were classified as low reliability (WR2 < 0.3). This implies that most transects have a moderate level of accuracy in the weighted linear regression.

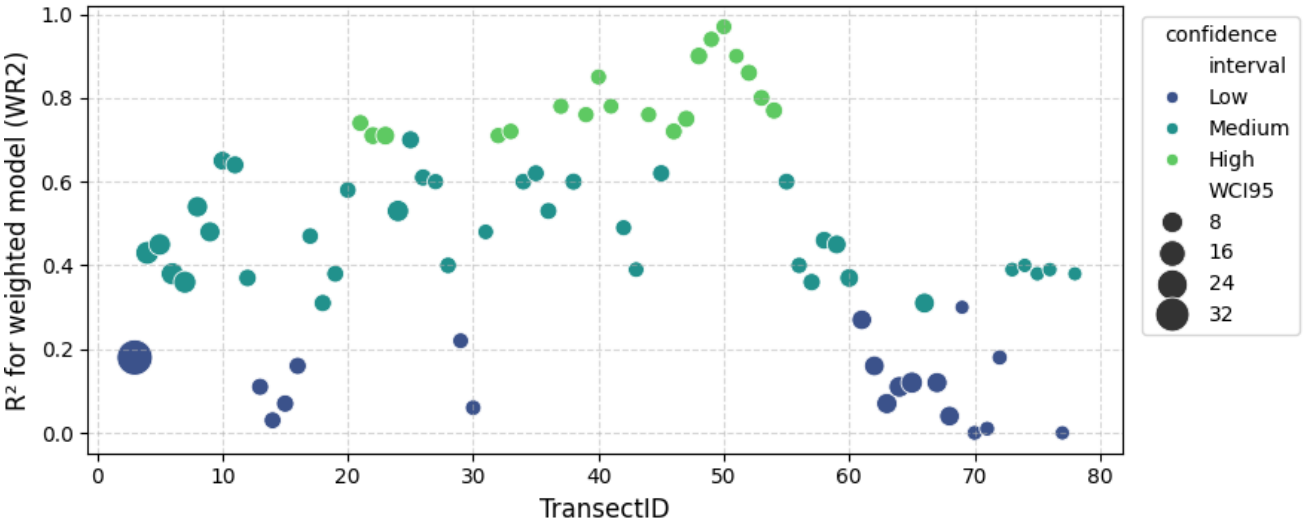

Figure 4. Reliability of the Weighted Linear Regression model (WR2 and WCI95) by transect

4.2. Coastline changes

The greatest deposition occurred in transect 4 (T4) in all methods. The EPR method suggests more intense erosion because it only considers the first and last dates (-1.54 m/year), while the LRR and WLR methods provide more stable estimates because they analyze all available dates (-1.24 m/year). Transect 23 is the most erosive in the EPR method, and transect 52 (T52) is the most erosive in the LRR (*Table 1*).

Table 1. Comparison of Coastline Change Rates

Method	Mean (m/yr)	Max. Erosion (m/yr)	Max. Deposition (m/yr)	% Erosion	% Deposition
EPR (End Point Rate)	-1.54	-11.06 (T23)	15.43 (T4)	67.9%	32.1%
LRR (Linear Regression Rate)	-1.24	-11.02 (T52)	8.78 (T4)	65.43%	34.57%
WLR (Weighted Linear Regression)	-1.24	-11.02 (T52)	8.78 (T4)	65.43%	34.57%

In *Figure 5*, WLR values represent the rate of shoreline change (m/year) over time in each transect analyzed. Negative values (-11.1 < WLR ≤ -3.0) correspond to areas with severe erosion, with -11.1 m/year being the most intense rate recorded. In contrast, positive values (3.0 < WLR ≤ 8.8) reflect depositional processes, evidencing shoreline advance in certain sectors. In the bar graph (Figure 5), this dynamic is visually represented by colors: red bars indicate erosion (negative values), while blue bars represent accretion (positive values).

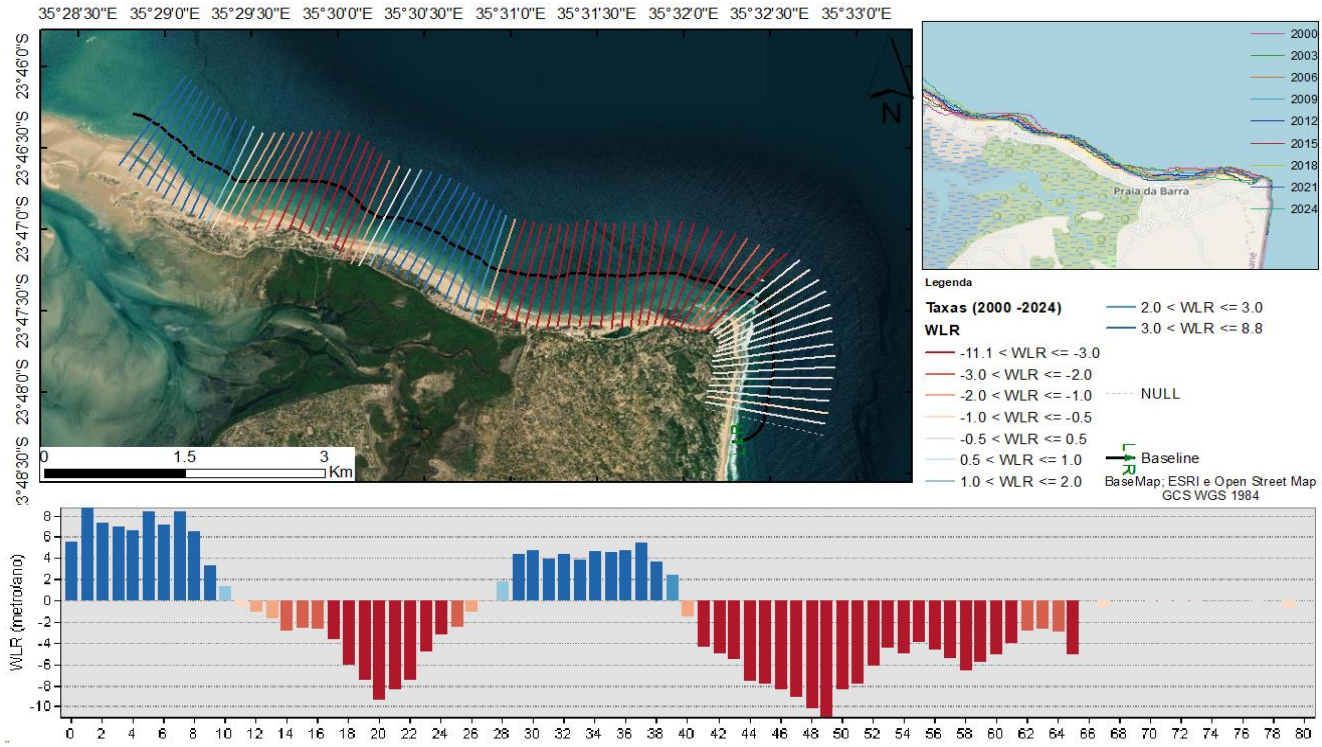

Figure 5. Weighted linear regression rate (WLR) for each transect analyzed on Barra beach.

Transects 52 to 55 (Latitude -23.7825 to -23.7827, Longitude 35.5249 to 35.5276) exhibit the largest magnitudes of negative WLR values, with rates ranging from -11.02 m/yr to -6.21 m/yr (Figure 5). These values indicate that these areas are retreating rapidly due to intensified erosion processes. However, transects at the beginning of the analysis, such as 3 to 11 (Latitude -23.7676 to -23.7717, Longitude 35.4852 to 35.4902), show positive WLR values (3.31 m/yr to 8.78 m/yr), indicating shoreline advance due to sedimentary deposition.

5. Discussion

Statistical analysis of the coastal dynamics at Barra Beach reveals a clear predominance of erosion, with an average rate of -2.72 m/year. It is important to note that the observed average retreat rate significantly exceeds the global average of approximately -0.5 m/year reported by Luijendijk et al. (2018), placing Barra Beach among the areas most vulnerable to coastal erosion internationally. In contrast, shoreline progradation occurs in 34.6% of transects (28 transects), with an average advance rate of 1.48 m/year. These results indicate a lower magnitude and lower variability associated with depositional processes when compared to erosion, reinforcing the asymmetric nature of local coastal dynamics, where erosion predominates over depositional trends.

A relevant aspect is the coincidence between the highest erosion rates and the presence of tourism infrastructure. This pattern suggests that the removal or absence of natural vegetation, especially dunes anchored by native vegetation, compromises the resilience of the shoreline, reducing its buffering capacity against the action of waves, tides, and winds (Figure 6). Azevedo et al. (2013) observed that, on Barra Beach, tourist accommodation units are located on primary dunes, sites where sea turtles nest cyclically and where different flora and fauna species inhabit. According to Palalane et al. (2016), construction in prohibited areas on Barra Beach, such as on primary dunes, impedes the natural recovery of the beach and increases the coast's vulnerability to erosion. Therefore, the prevalence of erosion suggests the need for strategic interventions to mitigate impacts and protect the most vulnerable areas.

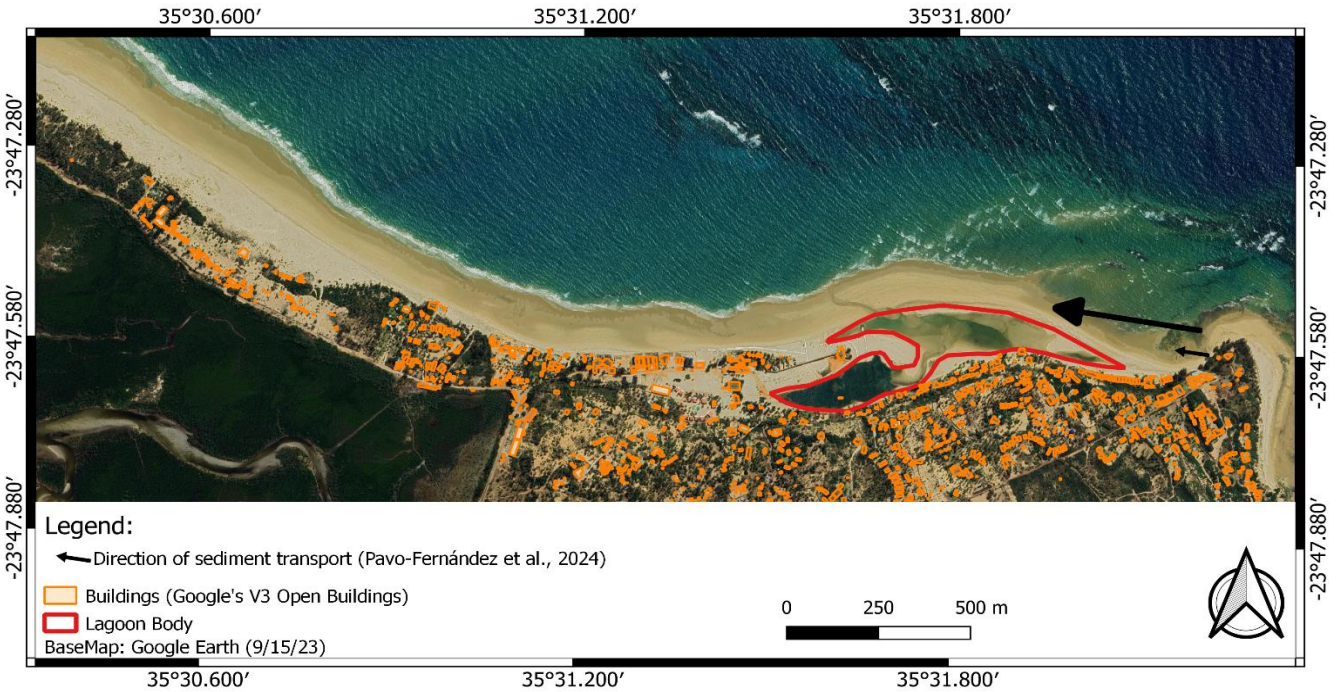

Figure 6. Aerial view of Barra Beach showing temporary lagoonal bodies and mobile sandbanks formed by longshore transport in the direction indicated by the arrow.

The Weighted Linear Regression Rate (WLR) results reinforce Azevedo's (2009) observations, indicating that tourism expansion on Barra Beach, particularly through the construction of facilities on dunes lacking coastal vegetation cover, plays a significant role in intensifying erosion. The analysis shows that the transects with the highest negative WLR rates are concentrated in areas of heavy human intervention, absence of native vegetation, and presence of tourism infrastructure. This pattern highlights that vegetation suppression compromises the natural stability of the dunes, reducing their barrier function against hydrodynamic agents and favoring the

advancement of the erosion process. Despite the anthropogenic influence, the general morphological behavior of the beach is marked by a juxtaposition of erosional and depositional sectors, reflecting a pattern of high spatial complexity. This alternation has already been documented on other high-energy coasts, such as the Kuwaiti coast (Aladwani, 2022) and the Yucatán Peninsula (Torres-Freyermuth et al., 2023).

The results obtained at Barra Beach are also consistent with the concept of shoreline self-organization (Coco; Murray, 2007), in which the dynamic interaction between waves and sediment transport generates alternating patterns of shoreline retreat and advance. Specifically, sedimentation was found to be more significant in the northwestern sector, which can be explained by the proximity to Inhambane Bay, which acts as a sediment source. Furthermore, northward longshore transport, favored by the predominance of southeasterly winds (Massuanganhe; Arnberg, 2008), conditions sediment redistribution along the region's beaches.

Another crucial point identified in this study is the importance of coastal vegetation in stabilizing the dunes and protecting them from the impacts of waves and winds. The reduced or absence of grasses and shrubs on Barra Beach increases the dunes' vulnerability to erosion. Vilanculo (2019) had previously reported significant sand mobility in the region, associated with the scarcity of vegetation and the occurrence of winds with speeds exceeding 6 m/s, capable of transporting sediment and intensifying wind erosion. The results also highlight the role of local hydrodynamic processes such as wave refraction, visible in the curvature of wave crests as they approach the coast. This evidence is reinforced by wind and surf statistics from the NWW3 model provided by Surf-Forecast (2025), which demonstrate the predominance of SSE-originating swells, with offshore winds occurring approximately 34% of the time and winds weak enough to leave the sea transparent in 11%.

From a coastal dynamics perspective, this directional predominance favors the concentration of wave energy in certain sectors of the beach, which can accentuate erosion processes already identified by Azevedo; Frei and Marques (2013). Longitudinal currents generated by SSE and offshore winds were identified as the main agents responsible for the evolution of the Pomene sandbar in Inhambane (Massuanganhe; Arnberg, 2008). These observations are corroborated by Pavo-Fernández; Gracia; Grifoll and Solana (2024), who describe Barra Beach as a highly energetic coastal system, characterized by intense longshore transport and high risk associated with wave and current action. Sediment movement indicates a transport pattern parallel to the shoreline, while wave incidence, often perpendicular to the beach, contributes to the alternation between erosion and deposition sectors. This behavior is consistent with the theory of Coco and Murray (2007), according to which coastal morphodynamics results from the continuous feedback between hydrodynamics and sediment transport, altering the coastline configuration over time.

5. Conclusions

This study analyzed the shoreline dynamics of Barra Beach, Inhambane province, over 24 years, integrating historical Landsat imagery, the Google Earth Engine platform, and the Digital Shoreline Analysis System (DSAS) tool. The results revealed that erosion predominates in 65.4% of the transects analyzed, with an average retreat rate of -2.72 m/year, higher than the global average. In contrast, deposition was observed in only 34.6% of the transects, with positive values reaching up to +8.8 m/year, particularly in the northern section of the beach, influenced by sediment input from Inhambane Bay and longitudinal transport. Areas with the highest negative weighted linear regression (WLR) values should be prioritized for future protection and mitigation actions. In addition to contributing to the understanding of local coastal dynamics, this study demonstrates the effectiveness of integrating Landsat imagery, Google Earth Engine, and DSAS as a low-cost, high-precision alternative for long-term coastline monitoring in Mozambique. Given this scenario, the implementation of sustainable coastal management measures in Barra Beach is urgently needed, especially in the stretches most affected by tourism.

Strategies such as restoring native vegetation, preserving dunes, and creating natural barriers can contribute to containing erosion, restoring coastal ecosystems, and improving the environmental resilience of the region and the country as a whole.

Author Contributions: Oldim Vilanculo: conception, methodology, formal analysis, manuscript preparation. Hélder Machaieie: conception, formal analysis, validation, manuscript review and editing. All authors have read and agreed to the published version of the manuscript.

Funding: This study was self-funded by the authors. No financial support was received from any organization or institution for this research.

Acknowledgments: We thank the two anonymous reviewers for their constructive comments and suggestions, which significantly improved the quality of the manuscript. We also thank Professor David G. Bowers (Bangor University, UK) for the linguistic review of the English version.

Conflict of Interest: The authors declare no conflict of interest.

References

1. ALADWANI, N. S. Shoreline change rate dynamics analysis and prediction of future positions using satellite imagery for the southern coast of Kuwait: A case study. **Oceanologia**, 64, n. 3, p. 417-432, 2022.
2. ALMONACID-CABALLER, J.; SÁNCHEZ-GARCÍA, E.; PARDO-PASCUAL, J. E.; BALAGUER-BESER, A. A. *et al.* Evaluation of annual mean shoreline position deduced from Landsat imagery as a mid-term coastal evolution indicator. **Marine Geology**, 372, p. 79-88, 2016.
3. AZEVEDO, H. A.; FREI, V. V. M.; MARQUES, A. C. D. O. Impactos e riscos ambientais da atividade turística: a Praia da Barra no Município de Inhambane/ Moçambique. vol. 15 nº2jul/dez, 2013, p. páginas: 1 –27, 2013/06 2013.
4. AZEVEDO, H. A. M. A. **Modelo de diagnóstico ambiental para elaboração do plano ambiental do município de Inhambane em Moçambique**. 2009. (Dissertação de Mestrado) - Universidade Católica de Brasília, Brasília.
5. BISHOP-TAYLOR, R.; NANSON, R.; SAGAR, S.; LYMBURNER, L. Mapping Australia's dynamic coastline at mean sea level using three decades of Landsat imagery. **Remote Sensing of Environment**, 267, p. 112734, 2021.
6. CABRAL, P.; AUGUSTO, G.; AKANDE, A.; COSTA, A. *et al.* Assessing Mozambique's exposure to coastal climate hazards and erosion. **International Journal of Disaster Risk Reduction**, 23, p. 45-52, 2017/08 2017.
7. CHRISTENSEN, K. H.; GAMMELSRØD, T.; HOGUANE, A.; TASKJELLE, T. *et al.* **A first assessment of nearshore waves and currents in Tofo, Inhambane**. Ministry for the Coordination of Environmental Affairs (MICOA), Mozambique. 2014.
8. CHRISTOFI, D.; METAS, C.; EVAGOROU, E.; STYLIANOU, N. *et al.* A Review of Open Remote Sensing Data with GIS, AI, and UAV Support for Shoreline Detection and Coastal Erosion Monitoring. **Appl. á Sci. á**, 15, p. 4771, 2025.
9. COCO, G.; MURRAY, A. B. Patterns in the sand: From forcing templates to self-organization. **Geomorphology**, 91, n. 3-4, p. 271-290, 2007.
10. CROWELL, M.; LEATHERMAN, S. P.; BUCKLEY, M. K. Historical shoreline change: error analysis and mapping accuracy. **Journal of coastal research**, p. 839-852, 1991.
11. DONCHYTS, G.; SCHELLEKENS, J.; WINSEMIUS, H.; EISEMANN, E. *et al.* A 30 m Resolution Surface Water Mask Including Estimation of Positional and Thematic Differences Using Landsat 8, SRTM and OpenStreetMap: A Case Study in the Murray-Darling Basin, Australia. **Remote Sensing**, 8, n. 5, p. 386, 2016/05/06 2016.
12. DUMOUCHEL, J.; HEES, F.; ALVIN, M. Coastal evolution and associated titanium sand mineralisation of Jangamo district, Inhambane Province, Mozambique. **Applied Earth Science**, 125, n. 3, p. 140-152, 2016.
13. ESTEVAM, C. N.; OSAKO, L. S.; FRANCISCO, J. A. A. Análise multitemporal da variação da linha de costa no setor centro-sul da Ilha de Santa Catarina, Brasil. **Geologia USP. Série Científica**, 21, n. 4, p. 73-90, 2021/12/14 2021.
14. FAN, D.; XU, J.; WU, Y.; LEE, G. H. Coastal environmental changes under increasing anthropogenic impacts: an introduction. **Anthropocene Coasts**, 2, n. 1, p. v-xii, 2019.

15. FERNANDO, M. **Políticas do turismo e a sustentabilidade sócioambiental em Moçambique: a experiência das áreas prioritárias para o investimento turístico e seus impactos no município de Inhambane**. 2013. 185 f. Dissertação (Mestrado em Desenvolvimento e Meio Ambiente) - Universidade Estadual da Paraíba.
16. FERREIRA, T. A. B. **Aplicação de sistema de análise de linha de costa (Digital Shoreline Analysis System) para avaliação de mudanças costeiras no delta do Parnaíba**. 2019. (Dissertação de Mestrado) -, Universidade Federal do Rio
17. Grande do Norte (UFRN), Brasil. Disponível em: https://repositorio.ufrn.br/jspui/handle/123456789/28519.
18. FORDYCE, A. J. Reef fishes of praia do Tofo and praia da Barra, Inhambane, Mozambique. **Western Indian Ocean Journal of Marine Science**, 17, n. 1, p. 71-91, 2018.
19. GORELICK, N.; HANCHER, M.; DIXON, M.; ILYUSHCHENKO, S. *et al.* Google Earth Engine: Planetary-scale geospatial analysis for everyone. **Remote Sensing of Environment**, 202, p. 18-27, 2017/12 2017.
20. GÜNEN, M. A.; ATASEVER, U. H. Remote sensing and monitoring of water resources: A comparative study of different indices and thresholding methods. **Science of the Total Environment**, 926, p. 172117, 2024.
21. HASTUTI, A. W.; ISMAIL, N. P.; NAGAI, M., 2024, **Analysis of coastline extraction indices using Sentinel-2 and Google Earth Engine, case study in Bali, Indonesia**. EDP Sciences. 04004.
22. HIMMELSTOSS, E. A.; HENDERSON, R. E.; FARRIS, A. S.; KRATZMANN, M. G. *et al.* **Digital Shoreline Analysis System version 6.0: U.S. Geological Survey software release**. 2024.
23. HOGUANE, A. M. Perfil diagnóstico da zona costeira de Moçambique. **Revista de Gestão Costeira Integrada-Journal of Integrated Coastal Zone Management**, 7, n. 1, p. 69-82, 2007.
24. HU, R.; FAN, Y.; ZHANG, X. Satellite-Derived Shoreline Changes of an Urban Beach and Their Relationship to Coastal Engineering. **Remote Sensing**, 16, n. 13, 2024.
25. IPCC. Summary for Policymakers. *In*: INTERGOVERNMENTAL PANEL ON CLIMATE, C. (Ed.). **Climate Change 2021 – The Physical Science Basis: Working Group I Contribution to the Sixth Assessment Report of the Intergovernmental Panel on Climate Change**. Cambridge: Cambridge University Press, 2021. p. 3-32.
26. JÚNIOR, W. C. G.; DE ALENCAR CASTRO, J. W. Variações Morfológicas e Erosão das Praias do Segmento Central do Estado do Rio de Janeiro: Técnicas de Sensoriamento Remoto e Padrões Granulométricos. **Geosciences= Geociências**, 43, n. 4, p. 633-644, 2024.
27. KELCHNER, H.; REEVE-ARNOLD, K. E.; SCHREINER, K. M.; BARGU, S. *et al.* Domoic Acid and Pseudo-nitzschia spp. Connected to Coastal Upwelling along Coastal Inhambane Province, Mozambique: A New Area of Concern. **Toxins**, 13, n. 12, p. 903, 2021.
28. LUIJENDIJK, A.; HAGENAARS, G.; RANASINGHE, R.; BAART, F. *et al.* The state of the world's beaches. **Scientific reports**, 8, n. 1, p. 6641, 2018.
29. MASSUANGANHE, E.; ARNBERG, W. Monitoring spit development in Pomene, southern Mozambique, using Landsat data. **WIT Transactions on The Built Environment**, 100, p. 119-127, 2008.
30. MATIAS, R. V. D. **Anthracological Analysis of Late Iron Age Shell-Middens Complex at Praia do Tofo and Praia da Rocha, Inhambane, Mozambique**. 2020. -, Universidade do Algarve (Portugal).
31. MUCHANGOS, A. D. Moçambique paisagens e regiões naturais. Maputo**:** 163 p p. 1999.
32. NGUYEN, H.-H.; MCALPINE, C.; PULLAR, D.; LEISZ, S. J. *et al.* Drivers of coastal shoreline change: case study of Hon Dat coast, Kien Giang, Vietnam. **Environmental management**, 55, n. 5, p. 1093-1108, 2015.
33. OKEMWA, E. The Implications of Climate Change and Sea Level Rise in the East African Coastal Region: a Study of Kenya. *In*: BORDOMER 92: International Convention on Rational Use of Coastal Zones; a preparatory meeting for the organization of an International Conference on Coastal Change, 1992, Bordeaux, France. Disponível em: http://hdl.handle.net/1834/7799.

34. OPPENHEIMER, M.; GLAVOVIC, B. C.; HINKEL, J.; VAN DE WAL, R. *et al.* Sea Level Rise and Implications for Low-Lying Islands, Coasts and Communities. *In*: INTERGOVERNMENTAL PANEL ON CLIMATE, C. (Ed.). **The Ocean and Cryosphere in a Changing Climate: Special Report of the Intergovernmental Panel on Climate Change**. Cambridge: Cambridge University Press, 2019. p. 321-446.
35. PAJAK, K.; IDZIKOWSKA, M.; KOWALCZYK, K. Sea Level Variability Assessment along the African Coast. **Sustainability**, 16, n. 13, p. 5661, 2024/07/02 2024.
36. PALALANE, J.; LARSON, M.; HANSON, H.; JUÍZO, D. Coastal erosion in Mozambique: Governing processes and remedial measures. **Journal of Coastal Research**, 32, n. 3, p. 700-718, 2016.
37. PARDO-PASCUAL, J. E.; SÁNCHEZ-GARCÍA, E.; ALMONACID-CABALLER, J.; PALOMAR-VÁZQUEZ, J. M. *et al.* Assessing the accuracy of automatically extracted shorelines on microtidal beaches from Landsat 7, Landsat 8 and Sentinel-2 imagery. **Remote Sensing**, 10, n. 2, p. 326, 2018.
38. PAVO-FERNÁNDEZ, E.; GRACIA, V.; GRIFOLL, M.; SOLANA, G. Longshore Sediment Transport Patterns In Mozambique: A Tool For Coastal Planning. : Copernicus GmbH 2024.
39. PRASAD, D. H.; KUMAR, N. D. Coastal Erosion Studies—A Review. **International Journal of Geosciences**, 05, n. 03, p. 341-345, 2014.
40. QUANG, D. N.; NGAN, V. H.; TAM, H. S.; VIET, N. T. *et al.* Long-Term Shoreline Evolution Using DSAS Technique: A Case Study of Quang Nam Province, Vietnam. **Journal of Marine Science and Engineering**, 9, n. 10, p. 1124, 2021/10/14 2021.
41. SAYRE, R.; NOBLE, S.; HAMANN, S.; SMITH, R. *et al.* A new 30 meter resolution global shoreline vector and associated global islands database for the development of standardized ecological coastal units. **Journal of Operational Oceanography**, 12, n. sup2, p. S47-S56, 2019.
42. SPINOSA, A.; ZIEMBA, A.; SAPONIERI, A.; DAMIANI, L. *et al.* Remote Sensing-Based Automatic Detection of Shoreline Position: A Case Study in Apulia Region. **Journal of Marine Science and Engineering**, 9, n. 6, p. 575, 2021/05/26 2021.
43. SURF-FORECAST. **Barra Beach Surf Stats**. 2025. Disponível em: https://pt.surf-forecast.com/breaks/Barra-Beach/surf-stats. Acesso em: 09 de Agosto de 2025.
44. TORRES-FREYERMUTH, A.; LÓPEZ-RAMADE, E.; MEDELLÍN, G.; ARRIAGA, J. A. *et al.* Assessing shoreline dynamics over multiple scales on the northern Yucatan Peninsula. **Regional Studies in Marine Science**, 68, p. 103247, 2023.
45. VILANCULO, G. D. J. D. **Estudo da Dinâmica Eólica Sedimentar das Dunas Costeiras na Praia de Barra, Cidade de Inhambane**. 2019. (Tese de Licenciatura) -, Universidade Eduardo Mondlane, Quelimane, Moçambique.
46. VOS, K.; SPLINTER, K. D.; HARLEY, M. D.; SIMMONS, J. A. *et al.* CoastSat: A Google Earth Engine-enabled Python toolkit to extract shorelines from publicly available satellite imagery. **Environmental Modelling & Software**, 122, p. 104528, 2019.
47. VOUSDOUKAS, M. I.; RANASINGHE, R.; MENTASCHI, L.; PLOMARITIS, T. A. *et al.* Sandy coastlines under threat of erosion. **Nature climate change**, 10, n. 3, p. 260-263, 2020.
48. XU, H. Modification of normalised difference water index (NDWI) to enhance open water features in remotely sensed imagery. **International Journal of Remote Sensing**, 27, n. 14, p. 3025-3033, 2006/07/20 2006.
49. ZACARIAS, D. A. **Vulnerabilidade comunitária às mudanças climáticas no município de Inhambane**. Centro de Desenvolvimento Sustentável para as Zonas Costeiras. Gaza, Moçambique. 2013.